

Climate-mediated dance of the plankton

Michael J. Behrenfeld

Climate change will unquestionably influence global ocean plankton because it directly impacts both the availability of growth-limiting resources and the ecological processes governing biomass distributions and annual cycles. Forecasting this change demands recognition of the vital, yet counterintuitive, attributes of the plankton world. The biomass of photosynthetic phytoplankton, for example, is not proportional to their division rate. Perhaps more surprising, physical processes (such as deep vertical mixing) can actually trigger an accumulation in phytoplankton while simultaneously decreasing their division rates. These behaviours emerge because changes in phytoplankton division rates are paralleled by proportional changes in grazing, viral attack and other loss rates. Here I discuss this trophic dance between predators and prey, how it dictates when phytoplankton biomass remains constant or achieves massive blooms, and how it can determine even the sign of change in ocean ecosystems under a warming climate.

Roughly one-half of the net primary production on Earth occurs in the ocean, yet the spatially integrated biomass of the dominant marine photoautotrophs, phytoplankton, is only around 1% of the plant biomass on land^{1,2}. The major contribution of phytoplankton (order 50 Pg C yr⁻¹) to biospheric production in part reflects the far greater area of the ocean and its less extreme seasonal cycles in growth conditions, but the stark contrast in total production-to-biomass ratios between land and ocean indicates a fundamental difference in system functioning. On average, the turnover time for the entire global phytoplankton biomass is a mere 2 to 6 days (refs 1,3), and across the vast subtropical gyres daily production is nearly perfectly matched by consumption and other losses (for example, cell lysis, sinking) throughout the year (that is, turnover ~1 day). Accordingly, the plankton world can exhibit trophic feedbacks, carbon cycling rates and climate sensitivities that behave very differently than many more familiar terrestrial systems where production of plant biomass can be decoupled from consumption over seasonal (for example, leaves in temperate deciduous forests) to multi-century timescales (for example, California Redwood).

Here, I provide a perspective on the counterintuitive nature of phytoplankton biomass and its temporal variability, with a particular focus on ocean regions exhibiting seasonal blooms (that is, periods of high biomass concentration). Phytoplankton blooms are 'hotspots' for fisheries production and play a vital role in atmosphere-ocean carbon dioxide exchange and the export of organic carbon to the deep sea⁴⁻⁷. The 'blooming process' is directly dependent on the physical properties of the upper ocean (for example, temperature, mixed-layer depth, seasonal stratification of the surface layer) that will be strongly modified by climate warming in the coming century, particularly at higher latitudes. However, the common view of how ocean physics is linked to phytoplankton biomass has been challenged by recent satellite, *in situ* and modelling studies⁸⁻¹¹. This issue is important because contrasting bloom hypotheses^{8,11-14} yield differences in even the sign of predicted future change in ocean biomass. One shortfall of the current debate has been its near-exclusive focus on bloom initiation, without sufficient context to biomass changes occurring before the initiation event or mechanisms connecting initiation to the bloom climax. Here, these issues are brought to the fore as critical constraints in identifying an emergent conceptual framework for understanding contemporary blooms and their susceptibility to climate change.

Before restricting this discussion to the blooming phenomenon, it is beneficial to 'step back' to the global domain and consider the basic properties of phytoplankton biomass, which herein refers to volumetric carbon concentrations (mg C m⁻³) unless specifically noted otherwise. Our ability to monitor phytoplankton properties at the global scale comes from satellite observations of ocean colour. These measurements detect spectral and intensity variations in light emerging from the surface ocean and allow assessment of basic ecosystem properties, including phytoplankton biomass and chlorophyll concentrations (mg m⁻³). Satellite data resolution is spatially (~1-5 km) and temporally (~1-8 day) coarser than field measurements, the detected signal does not register ecosystem properties below the actively mixed surface layer and little detail can currently be retrieved on the rich diversity of species comprising plankton communities. Nevertheless, understanding the observed temporal variability in these global satellite-derived properties can provide fundamental insights on how ocean ecosystems function and the processes guiding their temporal development.

Global phytoplankton fundamentals

The physical and chemical properties of the upper sunlit layer of the ocean are highly variable. In the central ocean gyres, this layer is clear, warm, strongly stratified, contains vanishingly low nutrient concentrations and receives high daily doses of sunlight throughout the year. By contrast, high-latitude regions in winter can have mixing depths of hundreds of metres, temperatures near 0 °C, little to no sunlight and very high nutrient concentrations. By mid-summer, these same regions may be converted to clear, warm and low nutrient waters with shallow surface-mixing depths and daily sunlight exposures comparable to low latitudes. Despite this tremendous diversity in upper-ocean conditions, surprisingly little variability is observed in the annual minima of phytoplankton biomass across the globe (Fig. 1a). Thus, the subarctic Atlantic annual minimum is comparable to equatorial regions, even though the subarctic population has experienced mixing to depths of hundreds of metres. This uniformity in biomass minima (Fig. 1a) is one indication that ecological processes, in concert with physical-chemical properties, are important determinants of phytoplankton biomass. Interestingly, although ocean ecosystem models can be tuned to reproduce these observed minima, we still do not fully understand the mechanisms defining the lower biomass threshold¹⁵. One possibility is that it represents a boundary below which further decreases

in phytoplankton stocks become limited by contact frequencies between predators and prey.

An important phytoplankton property that clearly does register global variability in environmental conditions is the annual biomass maximum (Fig. 1b; note that the colour scale in this panel corresponds to a biomass range threefold greater than in Fig. 1a). Major phytoplankton blooms are observed in regions where surface nutrients are at least periodically elevated^{16,17} and, notably, where strong physical forcings can disturb the balance between phytoplankton division and loss rates (for example, dilution of plankton populations by mixed-layer deepening, deep-water upwelling or riverine influx). In contrast to these blooming regions, biomass maxima are suppressed throughout the nutrient-impoorished and permanently stratified ocean (Fig. 1b), which corresponds approximately to waters with annual mean sea surface temperatures $>15^{\circ}\text{C}$ (equatorward of the black lines in Fig. 1b)^{18,19}.

A temptation always exists for drawing parallels between terrestrial and ocean ecosystems, such as referring to the oligotrophic gyres as ‘deserts of the ocean’ and bloom-forming regions as akin to tropical or temperate forests. Quantitatively, though, this depiction is misleading with regard to accumulations in phytoplankton biomass. From the data in Fig. 1a,b, a simple calculation can be made for the number of times phytoplankton populations must double to increase from their annual minimum to maximum concentration. The resultant distribution reveals a global range in required doublings that is largely constrained between only one and seven, inclusive of the major high-latitude bloom-forming regions (Fig. 1c).

What makes these low values even more remarkable is that the rise from minimum to maximum biomass often requires multiple months to achieve. In other words, phytoplankton blooms can arise from very slow rates of accumulation sustained over a long period of time^{8,11}.

Although phytoplankton biomass changes represent only a modest number of population doublings, these accumulations in stock wholly under-represent actual production. In the field, phytoplankton division rates can be remarkably rapid, in some cases equivalent to more than three doublings per day²⁰. The stark difference between division and biomass accumulation rates is resoundingly illustrated by comparing the number of doublings required to increase from minimum to maximum biomass (Fig. 1c) with the total number of cell divisions occurring over this same time interval (Fig. 1d; note, total divisions is a product of the daily division rate and the number of days between minimum and maximum biomass, where division rate is calculated as mixed-layer net primary production divided by mixed-layer phytoplankton carbon; see Supplementary Discussion). Recognizing that the colour scale for Fig. 1d (total divisions) spans a value range 20-fold greater than that in Fig. 1c (population doublings), this comparison illustrates that seasonal biomass changes account for only a small fraction of total production (this conclusion is robust to uncertainties in division-rate estimates), with the vast majority ($\sim 80\%$ to nearly 100%) of phytoplankton production being consumed or otherwise lost during the blooming period (Supplementary Discussion). Stated more pointedly, phytoplankton blooms represent a residual difference between two far larger,

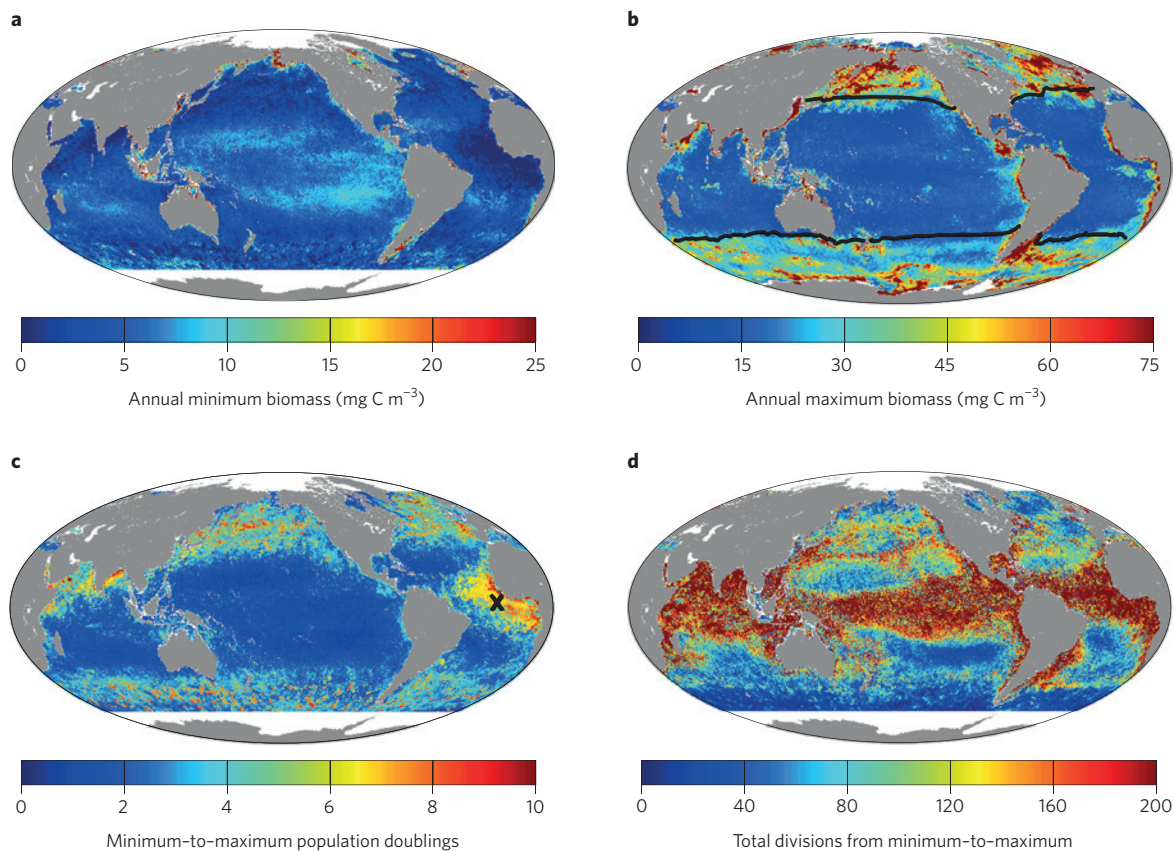


Figure 1 | Global dynamics of the phytoplankton biomass. **a, b**, Annual minima and maxima in phytoplankton biomass (mg C m^{-3}), respectively. **c**, Number of biomass doublings required to increase from the minimum values in **a** to the maximum values in **b**. **d**, Total number of phytoplankton cell divisions between the times of minimum and maximum concentration (total divisions = daily division rate \times days from minimum to maximum). Images are based on NASA MODerate-resolution Imaging Spectrometer (MODIS) 16-day average data for 2011. Phytoplankton biomass was calculated following ref. 66. Black lines in **b** correspond to annual mean sea surface temperatures of 15°C for 2011, which roughly delineates the permanently stratified oceans from higher-latitude, strongly seasonal regions. Note that the high doubling values west of equatorial Africa in **c** (marked by an 'X') are due to anomalously low values in **a** and may reflect uncertainties in satellite ocean retrievals in this region of high atmospheric aerosol (dust) loads.

but highly correlated terms: the rates of phytoplankton division and loss^{10,11,21–24}.

An additional, perhaps unexpected attribute of phytoplankton populations is that the total number of cell divisions between the biomass minimum and maximum (Fig. 1d) does not determine the location of major ocean blooms (Fig. 1b). Indeed, comparison of these two properties suggests, to first order, an inverse relationship. For example, total cell divisions in tropical oceans (where the dominant, small species divide nearly every day^{25,26}) can far exceed those at higher latitudes, but the tropical ocean regions are characterized by relatively stable biomass while the higher-latitude regions frequently support blooms. Thus, even from this global perspective, it is clear that phytoplankton accumulation is generally decoupled from how fast a given phytoplankton population is dividing. This decoupling implies that current trends in ocean biomass^{18,19,27} are not simply reflections of rapid or slow phytoplankton division rates. Moreover, it means that the response of phytoplankton biomass to climate warming will be governed by ecological factors in addition to the division-limiting effects of light, temperature and nutrient changes.

Rates and debates

Although a phytoplankton bloom is incontrovertibly understood as the condition of elevated biomass, the process of 'blooming' (that is, increasing from a low to high concentration) is an issue of competing rates. Let me briefly elaborate this point. During the annual cycle, a blooming phase is characterized by a period when the division rate of phytoplankton (μ ; d^{-1}) exceeds the rate of total losses (l ; d^{-1}) from zooplankton grazing, viral lysis and sinking out of the mixed layer. Thus, $\mu > l$ during blooming and the biomass accumulation rate, $r = \mu - l$, has a positive value. Thus, it is the sign of the rate term, r , that defines 'blooming', not the absolute value.

The most common explanation for temperate and high-latitude phytoplankton blooms is that they are initiated when light-driven increases in division rate surpass a critical threshold value²⁸. Because the depth of surface mixing is a primary determinant of daily light exposure for phytoplankton in these regions, this interpretation of blooms is referred to as the critical depth hypothesis (CDH). Its description can be found in most biological oceanography textbooks. The CDH's attribution of bloom initiation to a threshold value for μ arose during its original formalization from the simple assumption that loss rates can be treated as a constant²⁸. The appealing simplicity of the CDH is likely one reason for its long-standing popularity¹⁴, but as a scientific foundation for understanding phytoplankton blooms, it does not stand up to observations.

The CDH yields two very testable outcomes: (1) deep mixing and low incident sunlight cause phytoplankton biomass to decrease (that is, r is negative) before reaching the critical threshold and (2) the rate of increase in biomass following bloom initiation covaries linearly with the division rate (that is, $r = \mu - c$, where c is a constant). Today, mixed-layer phytoplankton properties are continuously monitored through satellite ocean colour measurements and *in situ* autonomous sensors. Analysis of these data for the subarctic Atlantic, a classic bloom-forming ocean region, has revealed that phytoplankton concentrations do not show a spring-time transition from decreasing to increasing biomass. Instead, they show that phytoplankton concentrations can begin rising as soon as the mixed layer stops deepening^{8–10}. In other words, these data do not support the notion of a critical mixing depth before which phytoplankton accumulation is prevented by light-limited cell division. Furthermore, the satellite data yield no correlation between phytoplankton division rate and the rate of change in mixed-layer phytoplankton abundance¹¹. These findings refute the CDH as a viable explanation for phytoplankton blooms and are supported by sustained *in situ* autonomous optical profiling float measurements and ecosystem modelling^{9,10}.

Dismissal of the CDH has resulted in an active debate to establish a revised interpretation of blooms. One key shortcoming of the traditional hypothesis was its neglect of known variability in phytoplankton loss rates. A strong correlation between phytoplankton division and loss rates would imply that food web interactions play a major role in determining bloom emergence. However, the allure of interpreting increasing biomass as an expression of rapid phytoplankton division rates is hard to resist. Accordingly, one side of the current bloom debate upholds this fundamental belief and has provided an alternative interpretation of the satellite data^{12,13,29}. Specifically, it has been noted that the initial rise in phytoplankton concentration at the end of mixed-layer deepening also coincides with a switch between positive and negative heat flux from the surface ocean. At this transition, convective mixing of the upper ocean is dampened and turbulent transport of phytoplankton from the surface to depth can become sufficiently slow relative to the cell division rate that surface biomass can increase. In other words, bloom initiation may be triggered by cessation of deep convective mixing and the crossing of a critical threshold in turbulent mixing. This critical turbulence hypothesis (CTH) also yields a very testable prediction: that phytoplankton loss rates exceed division rates before the late-winter switch in net heat flux. Satellite and sustained *in situ* measurements have now shown that mixed-layer-integrated phytoplankton biomass in the subarctic Atlantic often increases while convection is still actively deepening the mixed layer^{8–10}. These findings are inconsistent with the CTH as a robust explanation for phytoplankton blooms.

Ecological 'disturbance'

In the subarctic Atlantic, the winter transition from mixed-layer deepening to shoaling occurs around February. At this time, chlorophyll concentrations are at their annual minimum and, seaward of the continental margins, show little spatial variability across the basin (Fig. 2a). What makes this uniformity remarkable is its stark contrast to patterns in physical properties, particularly the depth of winter mixing (Fig. 2b). During late autumn and winter, convection deepens the mixed layer and dilutes surface phytoplankton populations with essentially phytoplankton-free water from below. This process should result in lower chlorophyll concentrations where mixing is deepest, yet this correspondence is not observed (Fig. 2a,b). The reason for this discrepancy is that phytoplankton concentration is always influenced by the balance between division and loss rates, and this balance is also tied to physical processes such as mixing.

Mixed-layer deepening, along with decreasing sunlight, causes phytoplankton division rates to slow during autumn in the subarctic Atlantic. Loss rates exceed division rates during this period, so phytoplankton concentrations decrease. The change in concentration, however, has the important consequence of decreasing density-dependent grazing and viral infection efficiencies (as an interesting side note, this effect of dilution on phytoplankton loss rates is the foundation for assessing grazing and division rates in the field³⁰ and is accounted for in ocean ecosystem models^{10,31}). The associated reduction in loss rates is further augmented by simultaneous concentration changes from physical dilution of the phytoplankton, grazer and viral populations. Thus, phytoplankton loss rates are mechanistically coupled to division rates and physics. By early winter, these feedbacks can reach a tipping point where decreases in loss rates are greater than the light-driven decreases in phytoplankton division rates. This point marks the beginning of the 'blooming phase', but interestingly it does not necessarily coincide with an increase in phytoplankton concentration. Instead, the initial population increase may be distributed over a growing volume of water by mixed-layer deepening. Thus, the depth-integrated biomass of the phytoplankton increases (Fig. 2c), while concentrations remain relatively constant (Fig. 2a)¹¹, an effect also noted in sustained

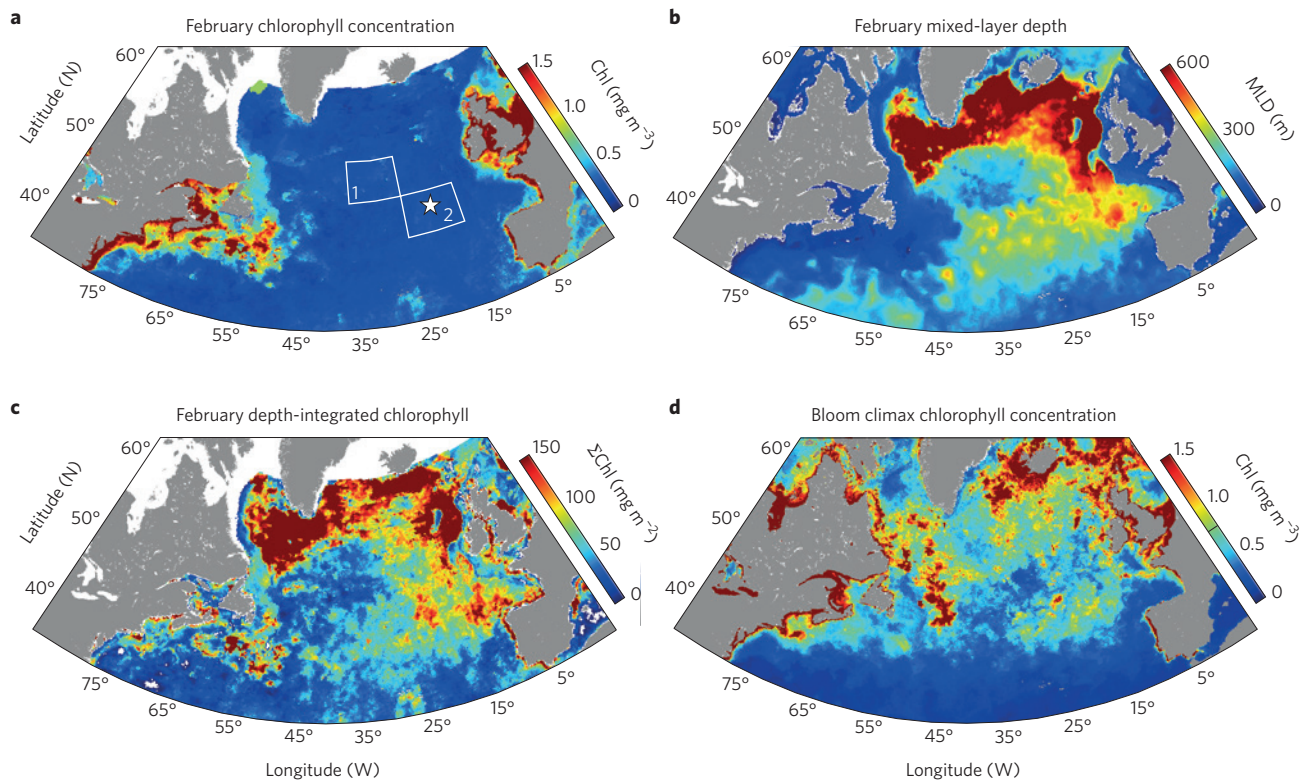


Figure 2 | Phytoplankton chlorophyll and winter mixed-layer depth in the subarctic Atlantic. **a**, February surface-chlorophyll concentration. **b**, February mixed-layer depth (MLD). **c**, February water-column chlorophyll inventory integrated from the surface to the MLD. **d**, Maximum chlorophyll concentration achieved during the spring/summer bloom climax. MLD data are from <http://www.science.oregonstate.edu/ocean.productivity/> and based on a data-assimilating physical ocean model, as described in ref. 10. White boxes in **a** show the location of data used in Figs 3 (Box 1) and 4 (Box 2). For reference, the location of the 1989 Joint Global Ocean Flux Study-North Atlantic Bloom Experiment (JGOFS-NABE)⁶⁷ is identified by the white star.

field measurements and modelling^{9,10}. So long as density-driven convection continues to deepen the mixed layer, phytoplankton can continue to accumulate in this manner without inducing a concentration-driven increase in density-dependent losses.

Although trophic feedbacks in plankton ecosystems are the dominant control on phytoplankton concentration³¹, physical disturbances to these feedbacks are also important. In the subarctic Atlantic, this link between physics and ecology allows water-column-integrated phytoplankton populations to increase in size while division rates are decreasing, with greater accumulations corresponding to deeper mixing (Fig. 2b,c). An important aspect of this relationship is its implication that dampened high-latitude winter mixing with climate warming will decrease annual maxima in depth-integrated phytoplankton biomass. For the subarctic Atlantic, this decrease has recently been estimated at an average of ~40% by the end of the coming century¹⁰.

The importance of physical disturbances to ecosystem structure and biomass is well established for intertidal, freshwater and terrestrial ecosystems^{32–35}, and clearly can be a governing factor in initiating open-ocean phytoplankton blooms. However, it provides little insight on the processes linking winter phytoplankton concentration minima (Fig. 2a) to concentration maxima at the bloom climax many months later (Fig. 2d). Understanding this bloom development over the spring stratification period requires further evaluation of plankton ‘predator–prey’ relationships.

New tools and new challenges

Arguably, the two most impactful developments in biological oceanography during the second half of the twentieth century were global satellite ocean colour measurements¹⁷ and the ability to conduct large-scale (on the order of 50 km²) purposeful manipulations of

natural plankton assemblages^{36,37}. These latter *in situ* experiments involved low-concentration additions of soluble iron to iron-limited surface phytoplankton populations. The initial outcome of such enrichments is a rapid rise in phytoplankton concentration, predominantly reflecting increases in species that were initially rare and presumably severely iron stressed^{36,38}. The second important outcome is that this blooming phase induced by iron addition only lasts for ~5 to 10 days before the enhanced phytoplankton division rates are either matched or overcome by escalating loss rates (that is, phytoplankton concentration stabilizes or decreases, respectively)^{11,36,39,40}. Recognizing that purposeful iron enrichments represent acute and major perturbations to plankton communities, this rapid response time of loss processes to changes in phytoplankton concentration is remarkable and in part reflects zooplankton with very rapid population growth rates²⁴. It also presents a challenging question for understanding natural blooms. If an increase in phytoplankton division rate can be overtaken by losses in 10 days or less, how can blooming in regions such as the subarctic Atlantic be sustained over periods of many months? The answer to this question is fundamental to predicting how climate-driven alterations of upper-ocean physical conditions, which vary slowly over the annual cycle relative to phytoplankton turnover rates, will impact plankton biomass stocks.

Ecological ‘recovery’

Physical processes can clearly interact with ecosystem feedbacks to initiate blooms (Fig. 2), but what happens when such forcings stop? When the disturbance ends, a critical consequence is that the existing difference between phytoplankton division and loss rates now causes phytoplankton concentrations to increase. This switch is documented in the satellite record for the subarctic Atlantic

by the coincident rise in phytoplankton carbon and chlorophyll concentrations with cessation of mixed-layer deepening^{8,10}. The new rise in concentration increases the encounter rate between phytoplankton and their predators (grazers, viruses), thereby enhancing predator populations and intensifying density-dependent losses^{10,11}. Purposeful iron-enrichment experiments suggest that this rise in loss rates should quickly curtail any further increases in the phytoplankton. However, there is a vital difference between artificial and natural blooms. Enrichment experiments cause phytoplankton division rates to increase from a low value to a higher value in a single-step function, which is soon matched by consumption rates. In contrast, division rates during natural, high-latitude blooms continue to increase throughout spring stratification, albeit often slowly⁸⁻¹¹. It is this continual rise in division rate that sustains the bloom to its climax^{11,31}. In other words, phytoplankton concentrations do not increase because of high division rates, but rather because division rates are accelerating. Conversely, decelerating division rates favour decreasing biomass. And, it is likely that this basic principle applies to phytoplankton biomass dynamics across the global oceans (Fig. 1) and will continue to operate under a warming climate.

The distinction between the 'division-rate' and 'ecosystem-feedback' interpretations of phytoplankton biomass cycles is well illustrated by subarctic Atlantic satellite data. The division-rate view is illustrated in Fig. 3a, which compares a climatological annual cycle in phytoplankton division rate (μ , green symbols) with measured rates of change in chlorophyll concentration (Δchl , red symbols; note the scale difference between the y axes; see ref. 10 for annual cycles in chlorophyll stocks for this region). Clearly, there is no resemblance in the annual cycles for these two properties and no critical division-rate threshold defining bloom initiation. Indeed, chlorophyll concentrations can increase ($\Delta\text{chl} > 0$) when division is extremely slow or decrease ($\Delta\text{chl} < 0$) when division rate is near maximal (Fig. 3a).

To illustrate the ecosystem-feedback view, one additional detail must be considered: the specific rate of change in biomass varies with the specific rate of change in division for planktonic systems operating near equilibrium^{11,31}. In other words, phytoplankton concentrations change in proportion to the relative change in μ , rather than the absolute change in μ . For example, an increase in division rate from 0.1 d^{-1} to 0.2 d^{-1} causes a larger increase in biomass than a rise from 0.5 d^{-1} to 0.6 d^{-1} . Or alternatively, a 20% increase in μ from 0.1 d^{-1} to 0.12 d^{-1} has a similar impact on biomass as a 20% increase from 0.5 d^{-1} to 0.6 d^{-1} , even though the absolute

change in μ is fivefold smaller in the former case. For eight-day resolution satellite data, the relative change in division rate ($\Delta\mu_{\text{rel}}$) is calculated as:

$$\Delta\mu_{\text{rel}} = \frac{(\mu_1 - \mu_0)}{(\mu_1 + \mu_0)/2} \quad (1)$$

where μ_1 is the division rate for one time point and μ_0 is the division rate eight days earlier. This calculation yields an annual cycle of $\Delta\mu_{\text{rel}}$ revealing basic drivers of Δchl variability (Fig. 3b). From late February to May, the spring bloom in phytoplankton concentration (Δchl , red symbols) corresponds to accelerating division rates (positive $\Delta\mu_{\text{rel}}$, blue symbols). Loss rates quickly catch up once division rates plateau near their summer maximum, and then drive a decrease in phytoplankton concentrations as μ decelerates into autumn. Around late November, the 'disturbance' phase of the cycle begins and continues until the mixed layer stops deepening around February. As discussed above, this phase initiates the bloom and allows phytoplankton concentrations to remain relatively constant despite strongly negative $\Delta\mu_{\text{rel}}$ (that is, note the November to February departure between red and blue symbols in Fig. 3b).

Recognizing blooms as consequences of highly correlated but slightly unbalanced changes in phytoplankton division and loss rates, rather than simply expressions of rapid division, has important implications regarding the impacts of climate variability. For example, if warming causes a decrease in winter mixing depths at high latitudes, then a division-centric view would suggest that the associated improvement in mixed-layer growth conditions would drive an earlier and, perhaps, stronger bloom⁴¹⁻⁴⁴. However, if the disturbance and recovery processes discussed here are correct, then the predicted outcome of shallower mixing is a later initiation of the blooming phase, a lower peak value in column-integrated phytoplankton biomass and potentially a weaker bloom climax, depending on whether the dampened annual cycle in μ is associated with lower values of $\Delta\mu_{\text{rel}}$ during spring stratification or a shorter blooming period^{10,11}.

Climate-mediated biomass variations

As voiced earlier³¹, the event of a bloom climax is perhaps less astonishing than the fact that the conditions necessary for a bloom are recreated each year. This recreation is imperfect, though, so the timing and magnitude of blooms varies from year to year. This variability is exemplified by a ten-year time series of satellite-observed

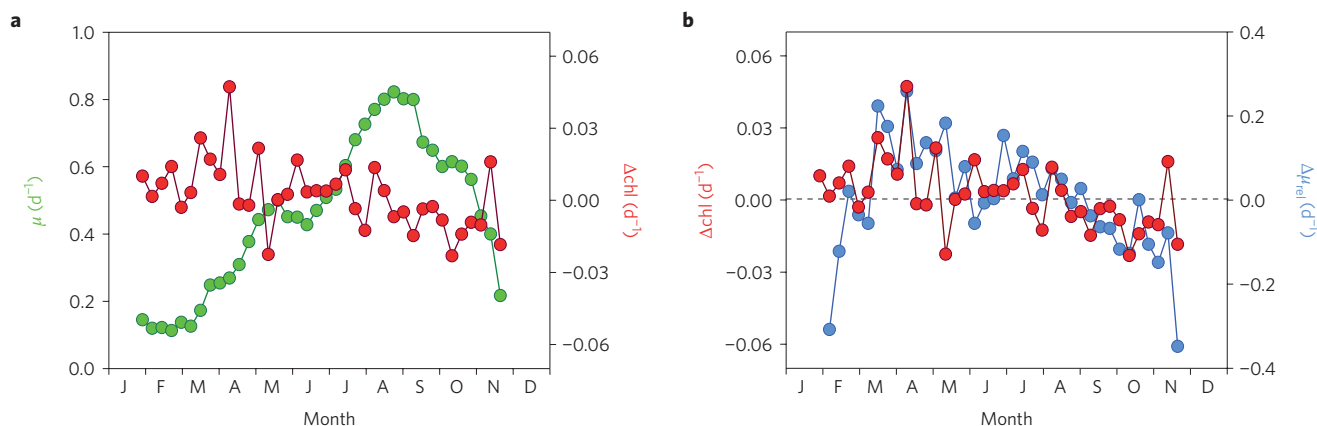


Figure 3 | Controls on phytoplankton accumulation rates. a, Climatological annual cycles in phytoplankton division rates (μ ; green, left axis) and observed rates of change in chlorophyll concentration (Δchl ; red, right axis). **b**, Climatological annual cycles in Δchl (red, left axis) and relative rates of change in phytoplankton division rate ($\Delta\mu_{\text{rel}}$; blue, right axis). Δchl is calculated as $\ln(\text{chl}_t/\text{chl}_0)/8$, where chl_t is chlorophyll concentration at a given time point and chl_0 is the chlorophyll concentration eight days earlier. $\Delta\mu_{\text{rel}}$ is calculated following equation (1) (see also Supplementary Discussion). Data correspond to the 5° latitude by 10° longitude bin outlined as Box 1 in Fig. 2a and are based on eight-day resolution chlorophyll products from the Sea-viewing Wide Field-of-view Sensor (SeaWiFS) for the period 1998 to 2008. At the latitude of this bin, no data are available from roughly December to mid-January.

phytoplankton chlorophyll and carbon concentrations for the subarctic Atlantic (Fig. 4a). The record exhibits a roughly fourfold range in bloom climax concentrations, but the time series for Δchl (Fig. 4b, red line) demonstrates that this interannual variability is due to very subtle differences in accumulation rates. This subtlety is less surprising, perhaps, when the full range in climax concentrations is recognized as representing a difference of only about two population doublings integrated over multiple months. Even so, these year-to-year differences have major consequences on year-class recruitment success for juvenile fish, food availability for higher-trophic-level migratory species and the flux of organic carbon to the deep sea^{45–49}.

The ecological underpinnings of biomass variability are again demonstrated by the satellite time series through the temporal correspondence between Δchl and $\Delta\mu_{\text{rel}}$ (Fig. 4b, blue line). This relationship is quite remarkable given that $\Delta\mu_{\text{rel}}$ largely reflects simple changes in light and mixed-layer conditions, includes errors associated with estimating daily photosynthesis from satellite data (for example, resulting from non-uniform distributions of phytoplankton through the water column; Supplementary Discussion), and does not account for the sinking of phytoplankton out of the surface mixed layer. What it implies is that accelerations and decelerations in the division rate function as primary drivers of biomass variability through their impact on predator–prey balances (Fig. 5). However, the outcome of this trophic feedback is complex. For example, the three largest blooms for the satellite record were each created differently. The large 1998 bloom was associated with a late-spring jump in $\Delta\mu_{\text{rel}}$, whereas in 1999 it reflected a prolonged period of positive but only modest $\Delta\mu_{\text{rel}}$. The 2001 bloom, in contrast, exhibited a large winter disturbance (black arrow), followed by progressively increasing $\Delta\mu_{\text{rel}}$ (Fig. 4b). This variability in contemporary ecosystem dynamics highlights the challenges inherent in predicting future climate-driven impacts, as the seasonal range in physical properties, their rate of change and the timing of this change all have implications for associated expressions in plankton stocks.

Dance of the plankton

A defining attribute of the plankton world is its tempo of feedback between trophic levels. Above all other factors, it is a propensity for rapid predator–prey re-equilibration that is responsible for the global divergence between phytoplankton biomass accumulation rates and division rates. From temperate to polar regions, spring-time increases in phytoplankton concentration are paralleled by the greening of deciduous forests at similar latitudes. But, this correlation is not indicative of similar causation. In the forest ecosystems, leaf production far outpaces leaf consumption, so rates of production and accumulation covary. For phytoplankton blooms, changes in loss rates are in close step with division rates, so this correspondence between accumulation and division disappears and relative rates of change become primary determinants of biomass variability.

In the current debate regarding controls on phytoplankton blooms, too much emphasis has been placed on bloom initiation without due consideration of biomass changes before and after this event. Hypotheses focused only on division-limiting, or ‘bottom-up’, factors (for example, CDH and CTH) fail to account for phytoplankton accumulations before their presumed threshold conditions, the absence of any correlation between division and accumulation rates, and the perpetuation of a bloom over its many months to climax^{12–14,29}. On the opposite side of the same coin has been an overemphasis on loss processes (particularly, zooplankton grazing), a view referred to as ‘top-down control’ of phytoplankton¹⁵. This interpretation fails to capture the dependence of annual phytoplankton biomass dynamics on relative accelerations and decelerations in phytoplankton division rate (Figs 3 and 4).

Consistent with ecosystem modelling results dating back to the 1940s^{21,22,50}, the interpretation of phytoplankton biomass variability requires a focus on the interactions between ‘bottom-up’ and ‘top-down’ processes (Fig. 5). From a framework of ecosystem ‘disturbance and recovery’ processes, annual biomass cycles throughout the global ocean can be seen as a dance between two intimate partners: phytoplankton division and their losses to predators. In the permanently stratified ocean, this dance is akin to the ‘Tango’.

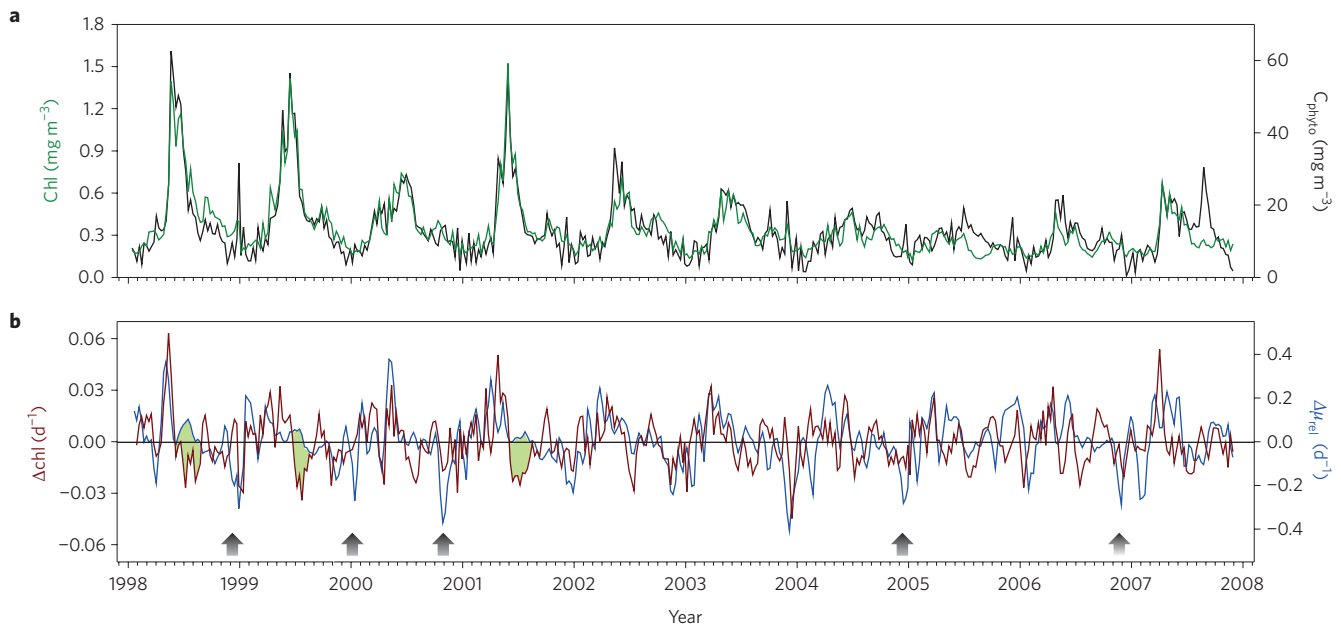


Figure 4 | A decade of variability in subarctic Atlantic phytoplankton concentrations. **a**, Eight-day resolution time series of phytoplankton chlorophyll (green; left axis) and carbon concentrations (black; right axis) corresponding to the 5° latitude by 10° longitude bin outlined as Box 2 in Fig. 2a. **b**, Corresponding time series of the rate of change in chlorophyll concentration (Δchl ; red, left axis) and the relative change in division rate ($\Delta\mu_{\text{rel}}$; blue, right axis). Black arrows mark winter ‘disturbance’ periods where observed chlorophyll changes are notably smaller than expected based on $\Delta\mu_{\text{rel}}$. Shaded green areas correspond to summer periods following the three largest blooms where observed changes in chlorophyll were notably larger than anticipated from $\Delta\mu_{\text{rel}}$. These discrepancies could reflect errors in calculated phytoplankton division-rate values due to post-climax iron stress^{68–70}.

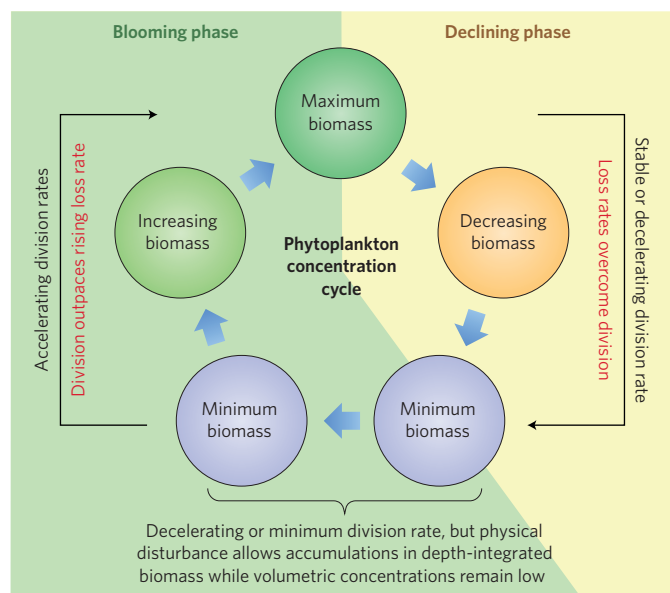


Figure 5 | Working framework for repeating cycles of phytoplankton biomass concentration. The ‘disturbance–recovery’^{10,11} cycle is delineated into a ‘blooming phase’ (green background) of increasing phytoplankton and a ‘declining phase’ (yellow background) of decreasing phytoplankton. Blooming is initiated by a disturbance in the predator–prey balance that allows phytoplankton division rates to first outpace loss rates. This disturbance may be a physical process, such as dilution of plankton populations through deep mixing, that results in an increased water-column-integrated phytoplankton stock without a change in concentration (blue to blue circles). Alternatively, it may be an improvement in growth conditions that causes phytoplankton division rates to accelerate (for example, iron-enrichment experiments). Once initiated, the blooming phase persists as long as division rates continue to accelerate (blue to light green to dark green circles). The bloom climax (dark green circle) occurs when division rates reach a maximum or begin to decline, allowing loss rates to overcome division rates. The subsequent ‘declining phase’ persists as long as division rates decelerate or a physical disturbance again tips the balance between division and loss rates.

Here, the dancers remain tightly coupled because growth conditions (that is, the ‘music’) change slowly over a constrained annual cycle. Bloom-forming regions in this analogy can perhaps be equated to the ‘Charleston’ dance, where partners are less tightly coupled because growth conditions vary over a wide dynamic range and on shorter timescales. In these regions, physical forcings can also be sufficiently severe to allow for the counterintuitive accumulation of depth-integrated biomass while phytoplankton division rates are still decelerating.

The dance of the plankton is continuously recorded by global satellite ocean colour measurements. From these data, an understanding can emerge of the choreography between the dancers and the music that will inform forecasts of ecosystem changes under a warmer climate. These insights will require careful attention to both partners in the dance and may also depend on resolving the complexities of plankton community composition. Here, I have treated plankton as a bulk property, with no regard for diversity, species succession or life history. This approach is not fully satisfying. Developments in omics capabilities^{51,52} and *in situ* technologies (for example, refs 53,54) now permit advanced characterization of taxonomic diversity and these observations are revealing a stunning and rapid succession of species dominance over the course of a bloom. Undoubtedly, the selective feeding behaviour of zooplankton plays a role in this phytoplankton succession^{55–57}, but the species specificity of this succession seems indicative of a major role for viruses^{58–60} and, potentially,

programmed cell death^{61,62}. The finer scale of field measurements compared with satellite data also reveals additional layers of spatial complexity in the evolution of plankton populations over the annual cycle. Resolving the mechanisms underlying these ecosystem dynamics and their significance to bloom development represents one of the major challenges for future research. Advanced remote-sensing capabilities, such as NASA’s upcoming PACE (Pre-Aerosol, Clouds, and ocean Ecosystem) mission, will contribute importantly to this end, but it will also require an integration of measurement and modelling approaches spanning a wide range of spatial and temporal scales, and resolving diverse plankton size domains and interactions^{11,63–65}.

Received 29 April 2014; accepted 22 July 2014; published online 25 September 2014

References

- Behrenfeld, M. J. & Falkowski, P. G. Photosynthetic rates derived from satellite-based chlorophyll concentration. *Limnol. Oceanogr.* **42**, 1–20 (1997).
- Field, C. B., Behrenfeld, M. J., Randerson, J. T. & Falkowski, P. G. Primary production of the biosphere: integrating terrestrial and oceanic components. *Science* **281**, 237–240 (1998).
- Antoine, D., André, J. M. & Morel, A. Oceanic primary production: II. Estimation at global scale from satellite (Coastal Zone Color Scanner) chlorophyll. *Glob. Biogeochem. Cycles* **10**, 57–69 (1996).
- Chassot, E. *et al.* Global marine primary production constrains fisheries catches. *Ecol. Lett.* **13**, 495–505 (2010).
- Takahashi, T. *et al.* Climatological mean and decadal change in surface ocean pCO₂ and net sea–air CO₂ flux over the global oceans. *Deep-Sea Res. II* **56**, 554–577 (2009).
- Alkire, M. B. *et al.* Estimates of net community production and export using high-resolution, Lagrangian measurements of O₂, NO₃⁻, and POC through the evolution of a spring diatom bloom in the North Atlantic. *Deep-Sea Res. I* **64**, 157–74 (2012).
- Siegel, D. A. *et al.* Global assessment of ocean carbon export by combining satellite observations and food-web models. *Glob. Biogeochem. Cycles* **28**, 181–196 (2014).
- Behrenfeld, M. J. Abandoning Sverdrup’s critical depth hypothesis on phytoplankton blooms. *Ecology* **91**, 977–989 (2010).
- Boss, E. & Behrenfeld, M. J. *In situ* evaluation of the initiation of the North Atlantic phytoplankton bloom. *Geophys. Res. Lett.* **37**, L18603 (2010).
- Behrenfeld, M. J., Doney, S. C., Lima, I., Boss, E. S. & Siegel, D. A. Annual cycles of ecological disturbance and recovery underlying the subarctic Atlantic spring plankton bloom. *Glob. Biogeochem. Cycles* **27**, 526–540 (2013).
- Behrenfeld, M. J. & Boss, E. S. Resurrecting the ecological underpinnings of ocean plankton blooms. *Annu. Rev. Mar. Sci.* **6**, 167–194 (2014).
- Taylor, J. R. & Ferrari, R. Ocean fronts trigger high latitude phytoplankton blooms. *Geophys. Res. Lett.* **38**, L23601 (2011).
- Taylor, J. R. & Ferrari, R. Shutdown of turbulent convection as a new criterion for the onset of spring phytoplankton blooms. *Limnol. Oceanogr.* **56**, 2293–2307 (2011).
- Mahadevan, A., D’Asaro, E., Lee, C. & Perry, M. J. Eddy-driven stratification initiates North Atlantic spring phytoplankton blooms. *Science* **337**, 54–58 (2012).
- Banse, K. Reflections about chance in my career, and on the top-down regulated world. *Annu. Rev. Mar. Sci.* **5**, 1–19 (2013).
- Sverdrup, H. U. The place of physical oceanography in oceanographic research. *J. Mar. Res.* **14**, 287–294 (1955).
- McClain, C. R. A decade of satellite ocean color observations. *Annu. Rev. Mar. Sci.* **1**, 19–42 (2009).
- Behrenfeld, M. J. *et al.* Climate-driven trends in contemporary ocean productivity. *Nature* **444**, 752–755 (2006).
- Siegel, D. A. *et al.* Regional to global assessments of phytoplankton dynamics from the SeaWiFS mission. *Remote Sens. Environ.* **135**, 77–91 (2013).
- Banse, K. Rates of phytoplankton cell division in the field and in iron enrichment experiments. *Limnol. Oceanogr.* **36**, 1886–1898 (1991).
- Riley, G. A. Factors controlling phytoplankton populations on Georges Bank. *J. Mar. Res.* **6**, 54–73 (1946).
- Riley, G. A. & Bumpus, D. F. Phytoplankton–zooplankton relationships on Georges Bank. *J. Mar. Res.* **6**, 33–47 (1946).
- Cushing, D. H. The seasonal variation in oceanic production as a problem in population dynamics. *J. Cons. Int. Explor. Mer.* **24**, 455–464 (1959).
- Banse, K. in *Primary Productivity and Biogeochemical Cycles in the Sea* (eds Falkowski, P. G. & Woodhead, A. D.) 409–440 (Plenum, 1992).

25. Vaulot, D., Marie, D., Olson, R. J. & Chisholm, S. W. Growth of *Prochlorococcus*, a photosynthetic prokaryote, in the equatorial Pacific Ocean. *Science* **268**, 1480–1482 (1995).
26. Vaulot, D. & Marie, D. Diel variability of photosynthetic picoplankton in the equatorial Pacific. *J. Geophys. Res.* **104**, 3297–3310 (1999).
27. Martinez, E., Antoine, D., D'Ortenzio, F. & Gentili, B. Climate-driven basin-scale decadal oscillations of oceanic phytoplankton. *Science* **326**, 1253–1256 (2009).
28. Sverdrup, H. U. On conditions for the vernal blooming of phytoplankton. *J. Cons. Int. Explor. Mer.* **18**, 287–295 (1953).
29. Chiswell, S. M. Annual cycles and spring blooms in phytoplankton: Don't abandon Sverdrup completely. *Mar. Ecol. Prog. Ser.* **443**, 39–50 (2011).
30. Landry, M. R. & Hassett, R. P. Estimating the grazing impact of marine micro-zooplankton. *Mar. Biol.* **67**, 283–288 (1982).
31. Evans, G. T. & Parslow, J. S. A model of annual plankton cycles. *Biol. Oceanogr.* **3**, 327–347 (1985).
32. Levin, S. A. & Paine, R. T. Disturbance, patch formation and community structure. *Proc. Natl Acad. Sci. USA* **71**, 2744–2747 (1974).
33. Menge, B. A. & Sutherland, J. P. Community regulation: variation in disturbance, competition, and predation in relation to environmental stress and recruitment. *Am. Nat.* **130**, 730–757 (1987).
34. Carpenter, S. R. & Kitchell, J. F. *The Trophic Cascade in Lakes* (Cambridge Univ. Press, 1993).
35. Terborgh, J., Feeley, K., Silman, M., Nuñez, P. & Balukjian, B. Vegetation dynamics of predator-free land-bridge islands. *J. Ecol.* **94**, 253–263 (2006).
36. de Baar, H. J. W. *et al.* Synthesis of iron fertilization experiments: from the Iron Age in the Age of Enlightenment. *J. Geophys. Res.* **110**, C09S16 (2005).
37. Boyd, P. W. *et al.* Mesoscale iron enrichment experiments 1993–2005: synthesis and future directions. *Science* **315**, 612–617 (2007).
38. Cavender-Bares, K. K., Mann, E. L., Chisholm, S. W., Ondrusek, M. E. & Bidigare, R. R. Differential response of equatorial Pacific phytoplankton to iron fertilization. *Limnol. Oceanogr.* **44**, 237–246 (1999).
39. Landry, M. R. *et al.* Biological response to iron fertilization in the eastern equatorial Pacific (IronEx II). III. Dynamics of phytoplankton growth and microzooplankton grazing. *Mar. Ecol. Prog. Ser.* **201**, 57–72 (2000).
40. Banse, K. Steemann Nielsen and the zooplankton. *Hydrobiologia* **480**, 15–28 (2002).
41. Bopp, L. *et al.* Potential impact of climate change on marine export production. *Glob. Biogeochem. Cycles* **15**, 81–99 (2001).
42. Boyd, P. W. & Doney, S. C. Modelling regional responses by marine pelagic ecosystems to global climate change. *Geophys. Res. Lett.* **29**, 53–1–53–4 (2002).
43. Sarmiento, J. L. *et al.* Response of ocean ecosystems to climate warming. *Glob. Biogeochem. Cycles* **18**, GB3003 (2004).
44. Henson, S. A., Dunne, J. P. & Sarmiento, J. L. Decadal variability in North Atlantic phytoplankton blooms. *J. Geophys. Res. Oceans* **114**, C04013 (2009).
45. Platt, T., Fuentes-Yaco, C. & Frank, K. Spring algal bloom and larval fish survival. *Nature* **423**, 398–399 (2003).
46. Edwards, M. & Richardson, J. Impact of climate change on marine pelagic phenology and trophic mismatch. *Nature* **430**, 881–884 (2004).
47. Koeller, P. *et al.* Basin-scale coherence in phenology of shrimps and phytoplankton in the North Atlantic Ocean. *Science* **324**, 791–793 (2009).
48. Lochte, K., Ducklow, H. W., Fasham, M. J. R. & Stienen, C. Plankton succession and carbon cycling at 47°N 20°W during the JGOFS North Atlantic Bloom Experiment. *Deep-Sea Res. II* **40**, 91–114 (1993).
49. Martin, P. *et al.* Export and mesopelagic particle flux during a North Atlantic spring diatom bloom. *Deep-Sea Res. I* **58**, 338–49 (2011).
50. Steele, J. H. *The Structure of Marine Ecosystems* (Harvard Univ. Press, 1974).
51. Teeling, H. *et al.* Substrate-controlled succession of marine bacterioplankton populations induced by a phytoplankton bloom. *Science* **336**, 608–611 (2012).
52. Vergin, K. L., Done, B., Carlson, C. A. & Giovannoni, S. J. Spatiotemporal distributions of rare bacterioplankton populations indicate adaptive strategies in the oligotrophic ocean. *Aquat. Microb. Ecol.* **71**, 1–13 (2013).
53. Olson, R. J. & Sosik, H. M. A submersible imaging-in-flow instrument to analyze nano- and microplankton: imaging FlowCytobot. *Limnol. Oceanogr. Meth.* **5**, 195–203 (2007).
54. Picheral, M. *et al.* The Underwater Vision Profiler 5: an advanced instrument for high spatial resolution studies of particle size spectra and zooplankton. *Limnol. Oceanogr. Meth.* **8**, 462–473 (2010).
55. Landry, M. R. Switching between herbivory and carnivory by the planktonic marine copepod *Calanus pacificus*. *Mar. Biol.* **65**, 77–82 (1981).
56. Verity, P. G., Smetacek, V. & Smayda, T. J. Status, trends and the future of the marine pelagic ecosystem. *Environ. Conserv.* **29**, 207–237 (2002).
57. Mariani, P., Andersen, K. H., Visser, A. W., Barton, A. D. & Kjørboe, T. Control of plankton seasonal succession by adaptive grazing. *Limnol. Oceanogr.* **58**, 173–184 (2013).
58. Suttle, C. A., Chan, A. M. & Cottrell, M. T. Infection of phytoplankton by viruses and reduction of primary productivity. *Nature* **347**, 467–469 (1990).
59. Vardi, A. *et al.* Viral glycosphingolipids induce lytic infection and cell death in marine phytoplankton. *Science* **326**, 861–865 (2009).
60. Bidle, K. D. & Vardi, A. A chemical arms race at sea mediates algal host-virus interactions. *Curr. Opin. Microbiol.* **14**, 449–457 (2011).
61. Berman-Frank, I., Bidle, K. D., Haramaty, L. & Falkowski, P. G. The demise of the marine cyanobacterium, *Trichodesmium* spp., via an autocatalyzed cell death pathway. *Limnol. Oceanogr.* **49**, 997–1005 (2004).
62. Bidle, K. D. & Falkowski, P. G. Cell death in planktonic, photosynthetic microorganisms. *Nature Rev. Microbiol.* **2**, 643–655 (2004).
63. Giovannoni, S. J. & Vergin, K. L. Seasonality in ocean microbial communities. *Science* **335**, 671–676 (2012).
64. Baird, M. E. Limits to prediction in a size-resolved pelagic ecosystem model. *J. Plankton Res.* **32**, 1131–1146 (2010).
65. Prowe, A. E. F., Pahlow, M., Dutkiewicz, S., Follows, M. & Oschlies, A. Top-down control of marine phytoplankton diversity in a global ecosystem model. *Prog. Oceanogr.* **101**, 1–13 (2012).
66. Behrenfeld, M. J., Boss, E., Siegel, D. A. & Shea, D. M. Carbon-based ocean productivity and phytoplankton physiology from space. *Glob. Biogeochem. Cycles* **19**, GB1006 (2005).
67. Ducklow, H. W. & Harris, R. P. Introduction to the JGOFS North Atlantic Bloom Experiment. *Deep-Sea Res. II* **40**, 1–8 (1993).
68. Blain, S. *et al.* Availability of iron and major nutrients for phytoplankton in the northeast Atlantic Ocean. *Limnol. Oceanogr.* **49**, 2095–2104 (2004).
69. Moore, C. M. *et al.* Phytoplankton photoacclimation and photoadaptation in response to environmental gradients in a shelf sea. *Limnol. Oceanogr.* **51**, 936–949 (2006).
70. Nielsdottir, M. C., Moore, C. M., Sanders, R., Hinz, D. J. & Achterberg, E. P. Iron limitation of the postbloom phytoplankton communities in the Iceland Basin. *Glob. Biogeochem. Cycles* **23**, GB3001 (2009).

Acknowledgements

This work was supported by the National Aeronautics and Space Administration's Ocean Biology and Biogeochemistry Program. I thank R. O'Malley for assistance with satellite data and analyses, and E. Boss, J. Graff, K. Halsey, B. Jones, A. Milligan and T. Westberry for helpful comments and discussions during the development of this manuscript.

Additional information

Supplementary information is available in the [online version of the paper](#). Reprints and permissions information is available online at www.nature.com/reprints. Correspondence and requests for materials should be addressed to M.J.B.

Competing financial interests

The author declares no competing financial interests.